

Hydration of Mononucleotides

Dengfeng Liu, Thomas Wyttenbach, and Michael T. Bowers*

Contribution from the Department of Chemistry and Biochemistry, University of California, Santa Barbara, California 93106

Received April 7, 2006; E-mail: bowers@chem.ucsb.edu

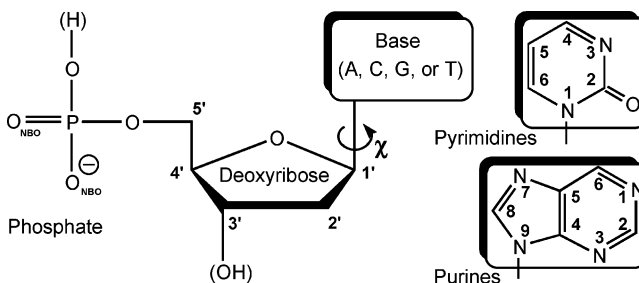
Abstract: The sequential addition of water molecules to protonated and deprotonated forms of the four mononucleotides dAMP, dCMP, dGMP, and dTMP was studied experimentally by equilibrium measurements using an electrospray mass spectrometer equipped with a drift cell and theoretically by computational methods including molecular modeling and density functional theory calculations. Experiments were carried out in positive and negative ion mode, and calculations included the protonated and deprotonated forms of the four nucleotides. For deprotonated anionic nucleotides the experimental enthalpies of hydration (ΔH^n) were found to be similar for all four systems and varied between -10.1 and -11.5 kcal mol $^{-1}$ for the first water molecule ($n = 1$) and -8.3 and -9.6 kcal mol $^{-1}$ for additional water molecules ($n = 2-4$). Theory indicated that the first water molecule binds to the charge-carrying phosphate group. Simulations of deprotonated mononucleotides with four water molecules yielded a large number of structures with similar energies. In some of the structures all four water molecules cluster around the phosphate group, and in other structures the four water molecules each hydrate a different functional group of the nucleotide. These include the phosphate group, the deoxyribose hydroxyl group, and various functional groups on the nucleobases. Experimental ΔH^1 values for the protonated cationic mononucleotides ranged from -10.5 to -13.5 kcal mol $^{-1}$ with more negative values (≤ -12 kcal mol $^{-1}$) for dCMP, dGMP, and dTMP and the least negative value for dAMP. For $n = 2-4$ the ΔH^n values varied from -6.9 to -9.7 kcal/mol and were similar in value to the deprotonated nucleotides except for dAMP. Theory on the protonated nucleotides indicated that the first water molecule binds to the charge-carrying group for dCMP, dGMP, and dTMP. For protonated dAMP, on the other hand, the charge-carrying N3 group is well self-solvated by the phosphate group and not readily available for a hydrogen bond with the water molecule. The insight gained on nucleotide stabilization by individual water molecules is used to discuss the competition between hydration of individual nucleotides and Watson–Crick base pairing.

Introduction

Deoxyribonucleic acid (DNA) research is at the heart of molecular biology, the science at the interface of biochemistry, cell biology, and genetics. The genetic information bearing DNA molecules form a double-stranded helix first proposed by Watson and Crick over 50 years ago.¹ Each DNA strand is a heteropolymer composed of repeating nucleotide units which in turn consist of a phosphate group, a deoxyribose sugar, and one out of the four nucleobases adenine (A), cytosine (C), guanine (G), and thymine (T) (Scheme 1). Polymerization of the DNA building blocks occurs via esterification of the 3' hydroxyl group with the phosphate of the adjacent nucleotide (see functional groups in parentheses in Scheme 1). The string of nucleotides is the text containing the genetic information written down by using the ACGT four-letter alphabet.

The adenine containing mononucleotide, the deoxyadenosine monophosphate, is denoted dAMP, with the other nucleotides correspondingly as dCMP, dGMP, and dTMP. Nucleotides are generally considered deprotonated in solution with the two nonbridging oxygen atoms O_{NBO} of the phosphate group carrying the negative charge (Scheme 1). Here we indicate

Scheme 1. Chemical Structure of Nucleotides Including Atom Numbering of Sugar, Purine Bases (A, G), and Pyrimidine Bases (C, T)



deprotonation explicitly (e.g., [dAMP-H] $^{-}$) to emphasize the nucleotide is a negative ion and to set it apart from the corresponding protonated positive ion (e.g., [dAMP+H] $^{+}$). One of the parameters defining the mononucleotide conformation is the dihedral angle about the N-glycosidic bond between the sugar and base (denoted χ in Scheme 1). The two possible orientations of the base with respect to the sugar are termed syn (base centered above sugar ring) and anti (base pointing away from sugar ring).

In the living organism DNA chemistry is carried out in solution where the negatively charged DNA molecules and

(1) Watson, J. D.; Crick, F. H. C. *Nature (London)* **1953**, *171*, 737.

mononucleotides interact very strongly with the polar water molecules. On the other hand, DNA molecules also interact very strongly with each other forming the extremely stable double-stranded helices, most often in a conformation called the B-form helix.² Hence, it is of paramount importance to understand the balance between the forces involved that make the complex biochemical processes work. This includes understanding the stabilization of biomolecules in their correct composition and conformation, such that they are able to take part in the biochemical processes. Our research effort is an attempt to quantify intramolecular and intermolecular forces and address issues such as those raised in the following questions. How does the interaction between two DNA strands compete with hydration of a single strand? What are the energetic contributions for each type of interaction? What are the hydration sites along DNA, and how strongly is water bound at each site? How do intermolecular interactions influence the biopolymer conformation?

Previous studies addressing the energetics of DNA hydration on a molecular level focused predominantly on water–nucleobase clusters. These studies include early field-ionization mass spectrometry experiments,³ cluster beam experiments,⁴ and theoretical work.^{5,6} In this study we investigate the interaction of individual water molecules with mononucleotides. The study includes both the protonated $[M+H]^+$ and the deprotonated $[M-H]^-$ form of the four nucleotides dAMP, dCMP, dGMP, and dTMP. Whereas nucleotides are typically negatively charged $[M-H]^-$ at physiological pH (see above, Scheme 1), positive ion $[M+H]^+$ hydration occurs under acidic electrospray conditions, and these studies complement the findings of the negative ions and provide additional insight into the hydration of the nucleobases.

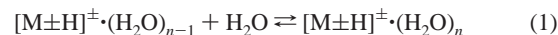
The present study on mononucleotides provides a basis for understanding hydration of the DNA polymer. However, the phosphate $-OH$ group and the 3' deoxyribose hydroxyl group of the monomer (shown in parentheses in Scheme 1) are not present in polymerized nucleotides, and hydration of these groups is unique to the monomer. In double-stranded DNA the bases are engaged in hydrogen bonds from one strand to the other forming the Watson–Crick base pairs and are not readily available for hydration. However, it is important to understand hydration of the bases as a competing process to base pairing. Future studies will be directed toward hydration of more complex DNA systems.

Experimental Methods

The experimental method used here is analogous to that previously used for peptides,⁷ and the instrument has previously been described in detail.⁸ Ions produced by nano-electrospray ionization (ESI) are focused by an ion funnel and injected into a drift cell filled with ~ 0.1 to 2.3 Torr of water vapor (no additional buffer gases added). Ions travel through the cell under the influence of a weak electric field ($5\text{--}10\text{ V cm}^{-1}$ at 1 Torr of H_2O) and quickly equilibrate with water vapor.

The cell temperature is increased and lowered by electrical heaters or a flow of liquid nitrogen, respectively, and is measured by a Pt resistor and three thermocouples in various places in and around the copper cell. The amount of water uptake is analyzed in the quadrupole mass filter following the drift cell. The experimental setup and tuning conditions near the exit of the cell are optimized to minimize perturbations of the equilibrium after the drift cell (efficient pumping, low fields, cell pressure yielding product-to-reactant ratio near unity).^{7–10}

In the hydration experiment, the following reaction is investigated.



Because the concentration of $[M\pm H]^\pm \cdot (H_2O)_n$ is proportional to the ion intensity I_n in the mass spectrum, the equilibrium constant of reaction 1 can be expressed by

$$K_n = \frac{[[M\pm H]^\pm \cdot (H_2O)_n] \cdot 760 \text{ Torr}}{[[M\pm H]^\pm \cdot (H_2O)_{n-1}] \cdot P(H_2O)} = \frac{I_n}{I_{n-1}} \cdot \frac{760 \text{ Torr}}{P(H_2O)} \quad (2)$$

where the pressure of water $P(H_2O)$ is measured by a Baratron connected to the drift cell. Equilibrium constants K_n , averaged over several measurements carried out at different water pressures at constant temperature, are converted into ΔG_n° (eq 3). Measuring ΔG_n° as a function of temperature T and evaluating a plot of ΔG_n° versus T (eq 4) yields values for the hydration enthalpy ΔH_n° (intercept) and entropy ΔS_n° (slope).

$$\Delta G_n^\circ = -RT \ln K_n \quad (3)$$

$$\Delta G_n^\circ = \Delta H_n^\circ - T\Delta S_n^\circ \quad (4)$$

Uncertainties for ΔH_n° and ΔS_n° are derived from the standard deviations of the linear least-squares fits to the experimental data.

All of the samples were purchased from Sigma (St. Louis, MO) and used without further purification. Samples were typically sprayed from an $\sim 100\ \mu\text{M}$ solution using a metal-coated glass tip in a nano-electrospray arrangement. The solvent used is a 1:1 mixture of water and acetonitrile with 1% acetic acid added for positive ion experiments.

Theoretical Methods

In an attempt to theoretically understand experimental trends, the hydration process has also been studied by computer simulations using molecular mechanics (MM) methods. For these studies, the AMBER 7 suite of programs has been employed together with the standard AMBER force field.¹¹ For each system of fully dehydrated, singly hydrated, or multiply hydrated molecules, 100 model structures are obtained by a simulated annealing protocol identical to that previously used.¹² In this process, an initial structure is energy minimized, run through a 30 ps molecular dynamics (MD) simulation at 800 K, cooled to 0 K through another 10 ps MD run, and energy minimized again. This final structure and its energy are saved. This structure is then used as the starting point for another annealing cycle. The resulting candidate structures are grouped based on their energies, conformations, and water binding sites.

The lowest energy structure of each group of dehydrated and singly hydrated molecules is used as the initial structure for density functional theory (DFT) optimization on the B3LYP/6-31G* level¹³ using the GAUSSIAN03 software package.¹⁴ For the deprotonated, singly

(2) Franklin, R. E.; Gosling, R. G. *Acta Crystallogr.* **1953**, *6*, 673.

(3) Sukhodub, L. F. *Chem. Rev.* **1987**, *87*, 589.

(4) Kim, S. K.; Lee, W.; Herschbach, D. R. *J. Phys. Chem.* **1996**, *100*, 7933.

(5) Zhanpeisov, N. U.; Leszczynski, J. *Struct. Chem.* **2001**, *12*, 121.

(6) Gonzalez, E.; Deriabina, A.; Teplukhin, A.; Hernandez, A.; Poltev, V. I. *Theor. Chem. Acc.* **2003**, *110*, 460.

(7) Liu, D.; Wyttenbach, T.; Barran, P. E.; Bowers, M. T. *J. Am. Chem. Soc.* **2003**, *125*, 8458.

(8) Wyttenbach, T.; Kemper, P. R.; Bowers, M. T. *Int. J. Mass Spectrom.* **2001**, *212*, 13.

(9) Kemper, P. R.; Bowers, M. T. *J. Am. Soc. Mass Spectrom.* **1990**, *1*, 197.

(10) Kebarle, P.; Searles, S. K.; Zolla, A.; Scarborough, J.; Arshadi, M. *J. Am. Chem. Soc.* **1967**, *89*, 6393.

(11) Kollman, P. A. et al. *AMBER 7*; University of California: San Francisco, CA, 2002.

(12) Wyttenbach, T.; von Helden, G.; Bowers, M. T. *J. Am. Chem. Soc.* **1996**, *118*, 8355.

(13) (a) Becke, A. D. *J. Chem. Phys.* **1993**, *98*, 5648. (b) Lee, C. T.; Yang, W. T.; Parr, R. G. *Phys. Rev. B* **1988**, *37*, 785.

(14) Frisch, M. J. et al. *GAUSSIAN 03*; Gaussian, Inc.: Pittsburgh, PA, 2003.

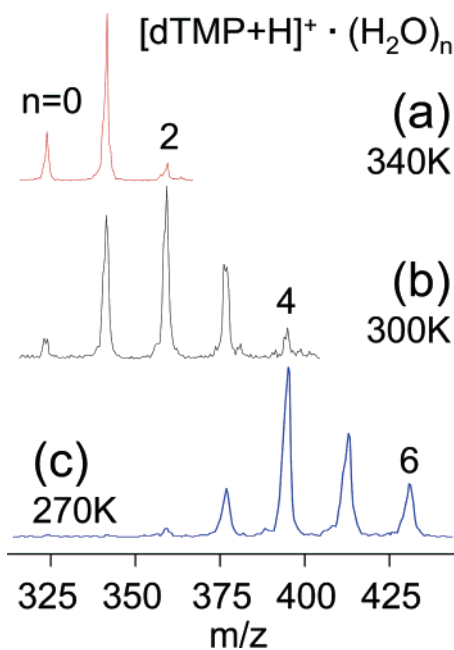


Figure 1. Mass spectra of protonated dTMP hydrated by n water molecules. Hydration equilibrium was established at 1 Torr of water vapor and a temperature of (a) 340 K, (b) 300 K, and (c) 270 K.

hydrated mononucleotides $[M-H]^- \cdot H_2O$, only one family of low-energy AMBER structures is found, and therefore the water binding energy of only one hydration site is evaluated by DFT methods. The AMBER result on singly hydrated protonated nucleotides $[M+H]^+ \cdot H_2O$ requires DFT-calculations for several hydration sites at the B3LYP/6-31G* level. All of the lowest energy B3LYP/6-31G* structures are further optimized at the B3LYP/6-311++G** level to obtain a more accurate water binding energy for comparison with experiment. Thermal energies are taken into account to obtain a value for the standard enthalpy at 298 K on the basis of a frequency calculation at the same level of theory as the optimization. All water-binding energies reported here are corrected by the counterpoise correction¹⁵ to account for basis set superposition errors (BSSE). No DFT calculations were carried out for ions hydrated by more than one water molecule.

This evaluation of candidate structures based on a simulated annealing protocol does not take entropy into account, even though the experiment samples structures favored by their *free* energy. We omitted entropy in our theoretical work to keep the calculations tractable. Ion mobility studies indicate that the structures of the types of systems studied here are predominantly determined by energy with entropy having a minor effect.^{16,17}

Results and Discussion

Experimental Results. Figure 1 shows a set of mass spectra obtained for $[dTMP+H]^+$ ions exposed to 1 Torr of water vapor at temperatures of 270 to 340 K. It can be seen that the number n of water molecules bound to the nucleotide increases with decreasing temperature. This is expected for an association reaction (eq 1) with loss of translational and rotational degrees of freedom and therefore with a negative $T\Delta S^\circ$ term. The temperature dependence shown in Figure 1 is typical for all protonated and deprotonated mononucleotides studied here.

Figure 2 summarizes the temperature dependence of the experimental data in terms of ΔG_n° values for the example of

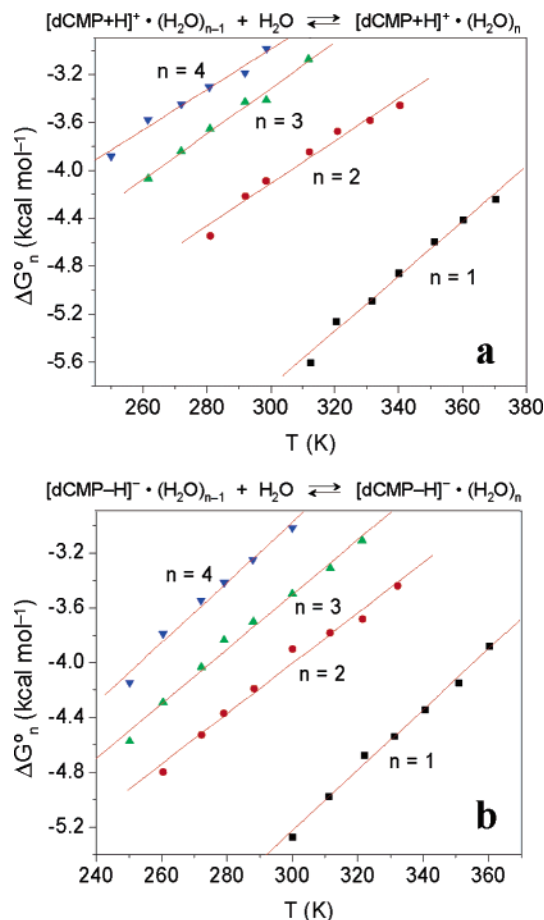


Figure 2. Plot of the free energy of hydration vs temperature measured for the (a) protonated and (b) deprotonated nucleotide dCMP.

Table 1. Experimental ΔH_n° and ΔS_n° Values^a for the Sequential Hydration (Eq 1) of Deprotonated and Protonated Mononucleotides

		$-\Delta H_n^\circ$ (kcal mol ⁻¹)				$-\Delta S_n^\circ$ (cal mol ⁻¹ K ⁻¹)			
		1	2	3	4	1	2	3	4
deprotonated	$[dAMP-H]^-$	10.3	9.4	9.3	8.6	19	18	19	18
	$[dCMP-H]^-$	11.5	9.5	9.5	9.6	22	18	20	22
	$[dGMP-H]^-$	10.9	8.3	9.1	9.2	23	16	20	21
	$[dTMP-H]^-$	10.1	9.0	9.2	8.8	19	17	20	20
protonated	$[dAMP+H]^+$	10.5	8.6	6.9	-	22	18	13	-
	$[dCMP+H]^+$	12.7	9.4	9.0	8.1	23	18	19	17
	$[dGMP+H]^+$	12.0	9.7	9.2	8.9	22	19	19	20
	$[dTMP+H]^+$	13.5	9.0	9.3	9.5	23	17	19	21

^a Uncertainty levels are ± 0.3 kcal mol⁻¹ for ΔH_n° , ± 1 cal mol⁻¹ K⁻¹ for ΔS_n° .

dCMP. Reliable data for addition of up to four water molecules are obtained in the temperature and water pressure range accessible. The corresponding ΔH_n° water binding energies and ΔS_n° entropies for all mononucleotides are listed in Table 1. In all cases the first water molecule is bound more strongly ($|\Delta H^\circ| > 10$ kcal mol⁻¹) than the following water molecules ($n = 2, 3, 4$). This effect is most pronounced for the positive ions $[dCMP+H]^+$, $[dGMP+H]^+$, and $[dTMP+H]^+$. The ΔH_n° values for $n = 2, 3$, and 4 are fairly constant at -9 ± 1 kcal mol⁻¹ for all positive and negative ions with the exception of $[dAMP+H]^+$.

The ΔS_n° values are strongly correlated with the corresponding ΔH_n° values. Analysis of the data in Table 1 yields the following correlation

(15) Boys, S. F.; Bernardi, F. *Mol. Phys.* **1970**, *19*, 553.

(16) Gidde, J.; Bowers, M. T. *Eur. Phys. J. D* **2002**, *20*, 409.

(17) Gidde, J.; Bowers, M. T. *J. Phys. Chem. B* **2003**, *107*, 12829.

$$\Delta S_n^\circ = \frac{2.0 \pm 0.2}{1000 \text{ K}} \Delta H_n^\circ \quad (5)$$

with smaller $\Delta S_n^\circ/\Delta H_n^\circ$ ratios ($\sim 0.0019 \text{ K}^{-1}$) on average for $n = 1$ and larger ratios ($\sim 0.0022 \text{ K}^{-1}$) for $n = 4$. It is not unexpected that ΔS_n° is correlated with ΔH_n° because a strong nucleotide–water interaction leads to both a large binding energy and a more rigid nucleotide–water complex with a large drop in entropy upon complex formation. A similar entropy–enthalpy correlation was observed for hydration of alkylamines, amino acids, and peptides.^{18,19} The smaller molecules of these systems containing an ammonium group were found to have average $\Delta S_n^\circ/\Delta H_n^\circ$ ratios of 0.0016 K^{-1} for $n = 1$ and 0.0020 K^{-1} for $n \geq 3$. The small value of 0.0016 K^{-1} for adding the first water molecule to an ammonium group indicates a relatively floppy ammonium–water complex in comparison to the nucleotide–water complex. In the ammonium–water complex the water molecule is bound by one hydrogen bond hardly restricting rotation about the water C_2 axis.¹⁸ The relatively large $\Delta S_1^\circ/\Delta H_1^\circ$ ratio of 0.0019 K^{-1} for the nucleotide–water complexes suggests that rotation of the water molecule is hindered in the complex possibly because of the presence of more than one hydrogen bond.

Structures of Deprotonated Nucleotides $[M-H]^- \cdot (H_2O)_n$

Previous ion mobility and theoretical work¹⁶ indicates that just one dominant family of structures exists for all four deprotonated mononucleotides. Figure 3a shows a typical representative of this family for the example dAMP. The conformation of the phosphate group and the sugar ring is the same for the other deprotonated nucleotides dCMP, dGMP, and dTMP, and all of them form the hydrogen bond between the 3' hydroxyl group on the sugar and the phosphate group shown in red in Figure 3a. The A, C, and T bases are rigid and planar and are attached to the deoxyribose system in an anti configuration as shown for dAMP in Figure 3a. However, the lowest energy dGMP structure has a syn sugar–base configuration and has an additional intramolecular hydration bond between the phosphate and its base guanine (Figure 4). Extensive theoretical studies of conformers relevant to the DNA structure yield identical sugar orientations even though the backbone is folded slightly differently.²⁰

For the singly hydrated ions AMBER results indicate that water binds preferentially to the charge-carrying phosphate group as expected. Water interacting with two phosphate oxygen atoms (Scheme 2, structure I) is found to be about equally stable to water forming just one linear hydrogen bond to the phosphate group (Scheme 2, structure II).

The presence of structure I with two hydrogen bonds explains the large $\Delta S_1^\circ/\Delta H_1^\circ$ ratio observed experimentally relative to the ammonium–water system with one hydrogen bond (see Experimental Results above).

In the case of dAMP, structure II is stabilized by a second hydrogen bond to the base as shown in Figure 3b. The calculated

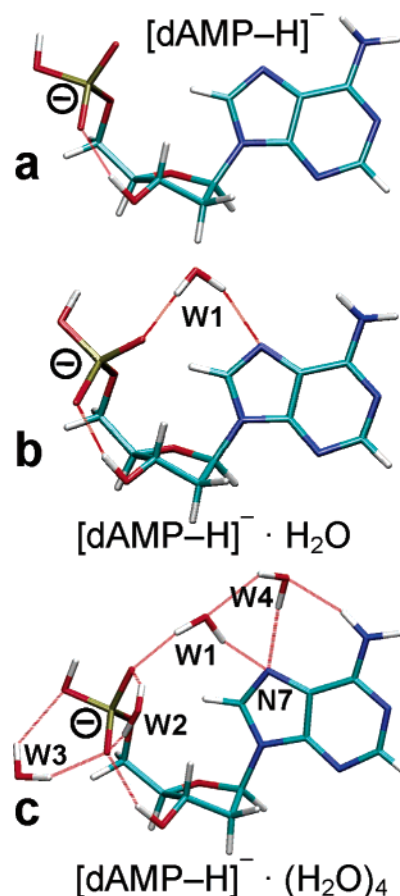


Figure 3. Geometry optimized structures of deprotonated dAMP: (a) fully dehydrated, (b) hydrated by one water molecule, (c) hydrated by four water molecules. The top two structures are the result of a full B3LYP/6-311++G** geometry optimization; the bottom structure is molecular mechanics (AMBER) based.

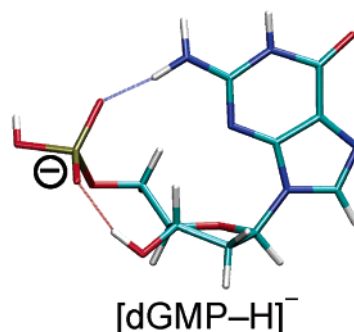
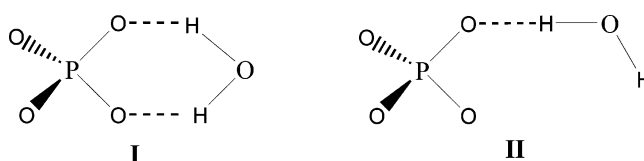


Figure 4. Geometry optimized structure of deprotonated dGMP calculated at the B3LYP/6-311++G** level.

Scheme 2



(B3LYP/6-311++G**) water binding energies are compiled in Table 2. It is apparent that the nature of the base has little effect on the binding energies in agreement with experiment. This is not surprising because the structure of the water–nucleotide complex $[M-H]^- \cdot H_2O$ is dominated by the water–phosphate interaction. The water–phosphate interaction in 2-deoxyribose

(18) Liu, D.; Wyttenbach, T.; Bowers, M. T. *Int. J. Mass Spectrom.* **2004**, *236*, 81.

(19) Wyttenbach, T.; Liu, D.; Bowers, M. T. *Int. J. Mass Spectrom.* **2005**, *240*, 221.

(20) (a) Shishkin, O. V.; Gorb, L.; Zhikol, O. A.; Leszczynski, J. *J. Biomol. Struct. Dyn.* **2004**, *22*, 227–243. (b) Gorb, L.; Shishkin, O. V.; Leszczynski, J. *J. Biomol. Struct. Dyn.* **2005**, *22*, 441. (c) Shishkin, O. V.; Palamarchuk, G. V.; Gorb, L.; Leszczynski, J. *J. Phys. Chem. B* **2006**, *110*, 4413.

Table 2. Theoretical^a (298 K) and Experimental ΔH°_1 Values (kcal mol⁻¹) for the Addition of One Water Molecule to Protonated and Deprotonated Mononucleotides

	calcd	expt		calcd	expt
[dAMP+H] ⁺	-11.4	-10.5	[dAMP-H] ⁻	-11.4	-10.3
[dCMP+H] ⁺	-12.6	-12.7	[dCMP-H] ⁻	-11.6	-11.5
[dGMP+H] ⁺	-12.4 ^b	-12.0	[dGMP-H] ⁻	-10.3	-10.9
[dTMP+H] ⁺	-14.6	-13.5	[dTMP-H] ⁻	-10.8	-10.1

^a B3LYP/6-311++G**. Structures given in Supporting Information.

^b Anti conformation (syn conformation: -12.0 kcal mol⁻¹). See text.

5-phosphate (no base) measured in our laboratory is 9.7 kcal mol⁻¹ in agreement with the mononucleotide values.

AMBER simulations of deprotonated mononucleotides hydrated by four water molecules yield a host of different isomers with similar energies. Some examples are shown in Figures 3c and 5a–d. The structures of Figures 3c and 5a, the lowest energy isomers of [dAMP-H]⁻·(H₂O)₄ and [dCMP-H]⁻·(H₂O)₄, respectively, are with three water molecules solvating the phosphate group examples of a common hydration pattern for all [M-H]⁻·(H₂O)₄ mononucleotide systems. The fourth, charge-remote, water molecule typically samples the best hydration site at the base. The charge-remote hydration site W4 for [dCMP-H]⁻·(H₂O)₄ (Figure 5a) is found to be the most favorable hydration site of the neutral base cytosine in a theoretical study.⁶ In the same study⁶ the adenine hydration site W4 (Figure 3c) is the preferred water binding site in the A·H₂O system. In another theoretical study on the adenine–water cluster A·(H₂O)₆ both positions W1 and W4 (Figure 3c) are found, although the orientation of W4 is slightly different from that shown in Figure 3c with the N7–W4 hydrogen bond missing.⁵

The [dCMP-H]⁻·(H₂O)₄ structures shown in Figure 5b–d are examples that illustrate the range of possible hydration patterns observed within 3 kcal mol⁻¹ of the global minimum. (AMBER energies are not expected to be more accurate than 3 kcal mol⁻¹.)¹⁸ Figure 5b shows extensive hydration of the phosphate group by four water molecules in the first hydration shell. One of the two charged nonbridging phosphate oxygen atoms O_{NBO} (see Scheme 1) is solvated by three water molecules W1–W3, and the other charged oxygen, by one water molecule W4 and by an intramolecular hydrogen bond to the sugar hydroxyl group. The structure shown in Figure 5c is characterized by an (H₂O)₃ cluster interacting with the phosphate group with two water molecules, W1 and W2, bound to the phosphate group (first solvation shell) and one water molecule W3 interacting with W1 and W2 (second solvation shell). The fourth water molecule W4 is bound to the base. In the [dCMP-H]⁻·(H₂O)₄ isomer shown in Figure 5d water binds in various places distributed over the entire molecule including the phosphate group (W1, W2), the sugar hydroxyl group (W2), and polar groups of the base (W3, W4).

The other mononucleotides show a very similar distribution of [M-H]⁻·(H₂O)₄ AMBER generated structures as shown in Figure 5 for dCMP. However, in dTMP the extent of base hydration is somewhat reduced and no structural analogue of that shown in Figure 5d with 2-fold base hydration was found for [dTMP-H]⁻·(H₂O)₄. The large number of near-isoenergetic isomers indicates that there are many different equally favorable water binding sites available to the second, third, and fourth water molecule, a result consistent with the experimental finding

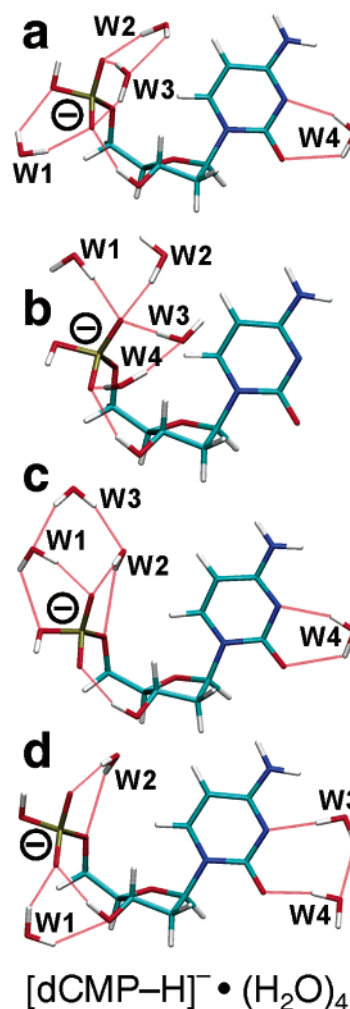


Figure 5. Low-energy structures of deprotonated dCMP hydrated by four water molecules obtained by molecular mechanics (AMBER) simulations. (a) Lowest-energy most typical structure, (b) isomer showing extensive phosphate hydration, (c) isomer with a water molecule in the second solvation shell, (d) isomer with water molecules bound to phosphate, sugar, and base.

of constant ΔH°_n values for $n = 2-4$ (Table 1). Since many of the [M-H]⁻·(H₂O)₄ isomers generated by AMBER include base hydration it can be concluded that the water–base interaction is ~ 9 kcal/mol (corresponding to $|\Delta H^{\circ}_n|$ for $n = 2$ to 4). The water–phosphate interaction energy is correspondingly 10–11 kcal mol⁻¹, given by $-\Delta H^{\circ}_n$ for $n = 1$.

A comparison of the various dehydrated and singly and multiply hydrated forms of mononucleotides indicates that the conformation of the nucleotide frame does not significantly change with hydration. The examples of [dAMP-H]⁻·(H₂O)_n structures shown in Figure 3a–c for $n = 0, 1,$ and 4, respectively, demonstrate how closely the nucleotide conformation is preserved during the first steps of hydration. Similarly, all of the [dCMP-H]⁻·(H₂O)_n structures of Figure 5 have almost identical dCMP conformations agreeing with the fully dehydrated molecule (not shown). The only notable difference between the various dCMP conformations is the orientation of the phosphate –OH group. The lowest energy –OH orientation of fully dehydrated [dCMP-H]⁻ corresponds to that of Figure 5a.

This remarkable conservation of conformation with hydration is in stark contrast to amino acids and peptides that undergo

significant structural changes upon addition of just a few water molecules.^{19,21–23} Those structural changes include substantial conformational adjustments and isomerization by proton transfer to form zwitterions. Dehydrated amino acids and small peptides are generally not zwitterions, whereas their fully hydrated counterparts generally are zwitterions. There is good evidence suggesting that the number of water molecules required to induce the neutral-to-zwitterion transition is very small.^{19,22,23} Some studies also suggest that addition of a small number of water molecules triggers conformational changes in amino acid side chains²¹ and in peptides.¹⁹

Structures of Protonated Nucleotides $[M+H]^+ \cdot (H_2O)_n$. As discussed in the previous section the preferred hydration sites of nucleotides are on the negatively charged phosphate groups with a water binding energy of 10–11 kcal mol⁻¹. However, our negative ion experiments indicate that the bases also offer fairly good hydration sites (9 kcal mol⁻¹). Those sites on the bases should also be available for hydration of positively charged nucleotides, and the water binding energy should be in the same range as that for the negative ions unless the base carries the positive charge of the nucleotide. Hence, it is interesting to evaluate the location of the positive charge and attempt to compare hydration experiments of the protonated mononucleotides $[M+H]^+$ with the results of the deprotonated counterparts.

Several research groups have addressed the issue of charge location on protonated mononucleotides and nucleobases both experimentally and theoretically.^{16,24} The conclusions of these studies are that the most likely sites of protonation are adenine N3 (see Scheme 1 for atom numbering) on dAMP, guanine N7 on dGMP, cytosine N3 on dCMP, and the phosphate group on dTMP. The present study is based on these findings.

An AMBER search for singly hydrated mononucleotide $[M+H]^+ \cdot H_2O$ structures of dCMP, dGMP, and dTMP shows that the first water molecule adds preferentially to the charged site as is the case for negative ions. However, the most favorable water binding site of $[dAMP+H]^+$ is on the phosphate group $-H_2PO_4$ even though the charge is located on the base. Figure 6 shows the structure of $[dAMP+H]^+$ and indicates that the phosphate group forms a hydrogen bond to the base at the site of protonation thereby effectively shielding the charge²⁵ and making it inaccessible to the water molecule. A space-filling model shows that the charge is fairly well buried in the interior of the molecule. Some of the charge is likely to transfer to the phosphate group making it the next best site of hydration.

However, the calculated water binding energy ($-\Delta H^{\circ}_1$) is smaller than that for the other protonated nucleotides in agreement with the experimental trend (Table 2). Other hydration sites for $[dAMP+H]^+$ (Table 3), though less favorable than the phosphate group, include the nucleobase amino group (second favorable site, W2 in Figure 6a) and the sugar hydroxyl

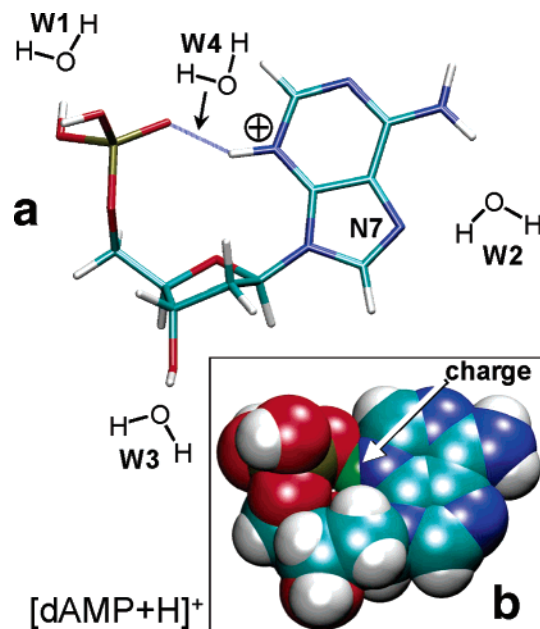


Figure 6. Geometry optimized structure of protonated dAMP (dehydrated) calculated at the B3LYP/6-311++G** level. (a) The primary hydration sites W1 through W4 with binding energies listed in Table 3 are schematically shown. The water molecule at site W4 inserts into the blue hydrogen bond between the proton on the base and the phosphate group thereby significantly changing the dAMP conformation (see text). (b) Space-filling representation of the same structure showing the efficient shielding of the charge. The proton involved in the hydrogen bond from the base to the phosphate (location of the charge) is highlighted in green.

Table 3. Theoretical^a ΔH°_1 (298 K) Values (kcal mol⁻¹) for the Addition of One Water Molecule to Protonated Mononucleotides at Various Sites^b

	phosphate	base		sugar
		protonation site	uncharged site	
$[dAMP+H]^+$	-12.5	-5.2	-9.6	-9.1
$[dCMP+H]^+$	-7.6	-15.4	N/A	-7.2
$[dGMP+H]^+$ (syn) ^c	-10.9	-16.5	-13.1	-7.4
$[dGMP+H]^+$ (anti) ^c	-13.3 ^d	-14.3	-13.2	-8.6
$[dTMP+H]^+$	-17.7	N/A	-9.4	-9.6

^a B3LYP/6-31G*. ^b The notation W1, W2, etc. in Figures 6 and 7 refers to the site with the most negative, second most negative, etc. ΔH°_n value. ^c dGMP in syn or anti conformation, respectively. See text. ^d Water (W3 in Figure 7b) is also bound to charge.

group (third favorable, W3). Water binding directly to the charge (W4) is also possible but requires the water molecule to insert into the base–phosphate hydrogen bond. This type of water insertion forces the nucleotide into an unfavorable conformation with a sugar–base orientation that is neither syn nor anti, and the resulting water binding energy is only 5.2 kcal mol⁻¹ (Table 3).

The W2 position, identical to W4 in Figure 3c, is the preferred hydration site in the A·H₂O system, as mentioned above, with a binding energy of 10.8 kcal mol⁻¹.⁶ This value, based on a carefully tuned force field calculation, is in good agreement with both an experimentally³ determined value for A·H₂O of 10.6 ± 1 kcal mol⁻¹ and our theoretical value of 9.6 kcal mol⁻¹ for this binding site (Table 3).

Modeling of $[dGMP+H]^+$ indicates that there are two different conformations with similar energies,²⁶ a compact structure with a syn sugar–base orientation leading to a hydrogen bond between the nucleobase amino group and the

- (21) Snoek, L. C.; Kroemer, R. T.; Simons, J. P. *Phys. Chem. Chem. Phys.* **2002**, *4*, 2130.
 (22) Xu, S. J.; Nilles, M.; Bowen, K. H. *J. Chem. Phys.* **2003**, *119*, 10696.
 (23) Lemoff, A. S.; Williams, E. R. *J. Am. Soc. Mass Spectrom.* **2004**, *15*, 1014.
 (24) (a) Smets, J.; Houben, L.; Schoone, K.; Maes, G.; Adamowicz, L. *Chem. Phys. Lett.* **1996**, *262*, 789. (b) Russo, N.; Toscano, M.; Grand, A.; Jolibis, F. *J. Comput. Chem.* **1998**, *9*, 989. (c) Green-Church, K. B.; Limbach, P. A. *J. Am. Soc. Mass Spectrom.* **2000**, *11*, 24. (d) Green-Church, K. B.; Limbach, P. A.; Freitas, M. A.; Marshall, A. G. *J. Am. Soc. Mass Spectrom.* **2001**, *12*, 268.
 (25) “Charge” refers to the partial charge δ^+ (<1.0) on the hydrogen atom H3. The total ionic charge +1 is distributed over the entire molecule with increased positive charge density centered at N3, N9, and the exocyclic $-NH_2$ group according to resonance structures.

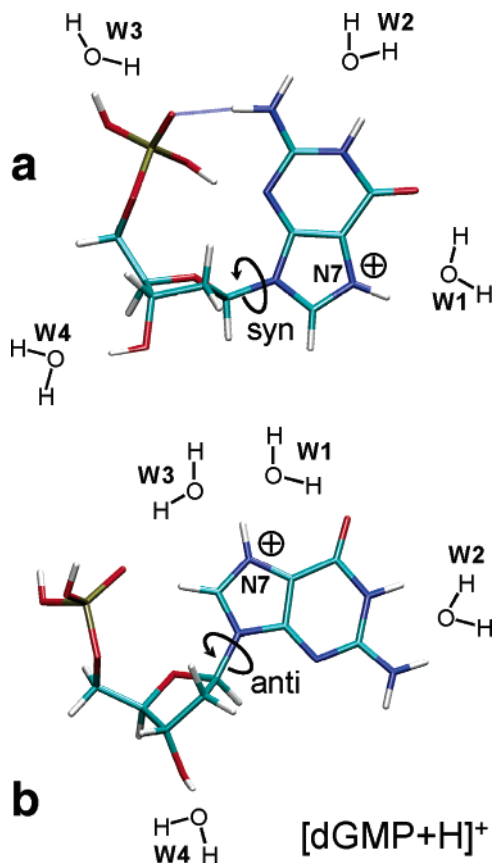


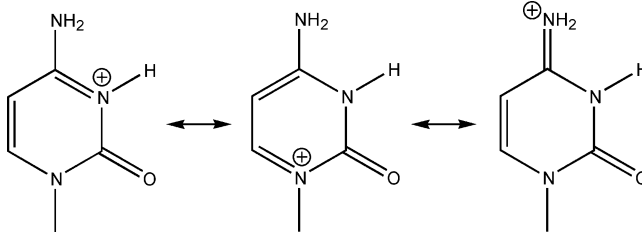
Figure 7. Geometry optimized structures of two protonated dGMP conformers (both dehydrated) with a (a) syn and (b) anti sugar–base orientation calculated at the B3LYP/6-311++G** level. The primary hydration sites W1 through W4 with binding energies listed in Table 3 are schematically shown.

phosphate group (Figure 7a) and a more open structure with an anti sugar–base orientation and no base–phosphate hydrogen bond (Figure 7b).¹⁶ The most favorable water binding site (W1) for both conformations is the protonated aromatic nitrogen group (N7) on the base, followed by water binding sites in charge remote locations on the base (W2), on the phosphate group (W3), and on the sugar (W4). Calculated water binding energies for the various binding sites identified in Figure 7 are compiled in Table 3.

The water binding site W2 is also found in other theoretical studies^{5,6} on neutral base–water systems, $G \cdot (H_2O)_n$, and with a $12.2 \text{ kcal mol}^{-1}$ binding energy is the second most favorable site in $G \cdot H_2O$.⁶ The best hydration site in $G \cdot H_2O$ ($12.4 \text{ kcal mol}^{-1}$) is near W1,⁶ not comparable to the $GH^+ \cdot H_2O$ system shown in Figure 7 because of the proximity of the charge. However, our charge-remote W2 binding energy of $13.1 \text{ kcal mol}^{-1}$ (Table 3) side by side with the $G \cdot H_2O$ force-field-based⁶ W2 value of $12.2 \text{ kcal mol}^{-1}$ is a fair comparison yielding good agreement. The experimental $G \cdot H_2O$ binding energy is $14.1 \pm 1 \text{ kcal mol}^{-1}$.³

Water binding energies of $[dTMP+H]^+$ are interesting for comparison with the deprotonated mononucleotides $[M-H]^-$ because the charge is located on the phosphate group in all cases ($-H_3PO_4^+$ and $-HPO_4^-$, respectively). Theory indicates that

Scheme 3. Resonance Structures of Protonated Cytosine



the first water molecule adds preferentially to the charged phosphate group for both $[dTMP+H]^+$ and $[M-H]^-$. The calculated water binding energies are 14.6 and $\sim 11 \text{ kcal mol}^{-1}$ (Table 2), respectively, in good agreement with the experimental values of 13.5 and $\sim 10 \text{ kcal mol}^{-1}$ (Table 2). It has previously been observed for peptides and other molecules that water interacts generally more strongly with positive RNH_3^+ ions than with negative $RCOO^-$ ions.¹⁹ For instance ΔH°_1 values for $CH_3(CH_2)_9NH_3^+$ and $CH_3(CH_2)_8COO^-$ are -14.8 and $-13.0 \text{ kcal mol}^{-1}$, respectively.¹⁹ The larger water binding energy of cations is presumably a result of the strong charge–dipole interaction due to a fairly tight ion charge distribution. The charge distribution of anions, on the other hand, is much more diffuse with the negative charge spread out in large orbitals (see, e.g., ionic radius of 1.33 \AA for F^- vs 1.02 \AA for Na^+ ²⁷).

Water binding energies calculated for charge-remote sites on $[dTMP+H]^+$ are several kilocalories per mole smaller than that for the $-H_3PO_4^+$ group (Table 3). Similarly the experimental $|\Delta H^{\circ}_n|$ values, $n = 2-4$, of 9 kcal mol^{-1} are significantly smaller than $|\Delta H^{\circ}_1|$ (Table 1) and compare very favorably with the ΔH°_n values, $n = 2-4$, of the deprotonated nucleotides. This is expected because the charge-remote hydration sites in $[dTMP+H]^+$ and $[dTMP-H]^-$ should be the same. AMBER simulations of the $[dTMP+H]^+ \cdot (H_2O)_4$ system indicate that on average two water molecules bind to the phosphate group and one water molecule each binds to the base and the sugar.

In summary, the experimental ΔH°_1 values for $[M+H]^+$ range from $-10.5 \text{ kcal mol}^{-1}$ for dAMP to $-13.5 \text{ kcal mol}^{-1}$ for dTMP. Theory tracks these values (-11.4 for dAMP, $-14.6 \text{ kcal mol}^{-1}$ for dTMP) and provides an explanation for the trends: The water binding energy of $[dAMP+H]^+$ is exceptionally small because the water molecule is not able to bind directly to the charge due to an existing intramolecular hydrogen bond involving the charged group. The dTMP value is larger than average because the positive charge does not sit on the base as is the case for the other mononucleotides but on the phosphate group. Partial charge delocalization over the entire base as shown in Scheme 3 for the example of cytosine weakens the protonated nucleobase–water interaction compared to the protonated phosphate–water interaction.

Water's ability to form two hydrogen bonds in nearly all hydration sites of protonated mononucleotides (see, e.g., Figures 6 and 7) suggests formation of relatively rigid nucleotide–water complexes in agreement with experimental $\Delta S^{\circ}_1/\Delta H^{\circ}_1$ ratios which are larger than those in ammonium–water systems¹⁸ with one hydrogen bond (see Experimental Results).

Hydration of DNA. The DNA-polymer molecule typically combines with a second polymer strand with complementary

(26) The syn structure is calculated to be 0.9 and $3.0 \text{ kcal mol}^{-1}$ higher in energy than the anti structure at the B3LYP/6-31G* and B3LYP/6-311++G** level of theory, respectively.

(27) Lide, D. R., Ed. *CRC Handbook of Chemistry and Physics*, 85th ed.; CRC: Boca Raton, FL, 2004; <http://www.hbcnpnetbase.com>

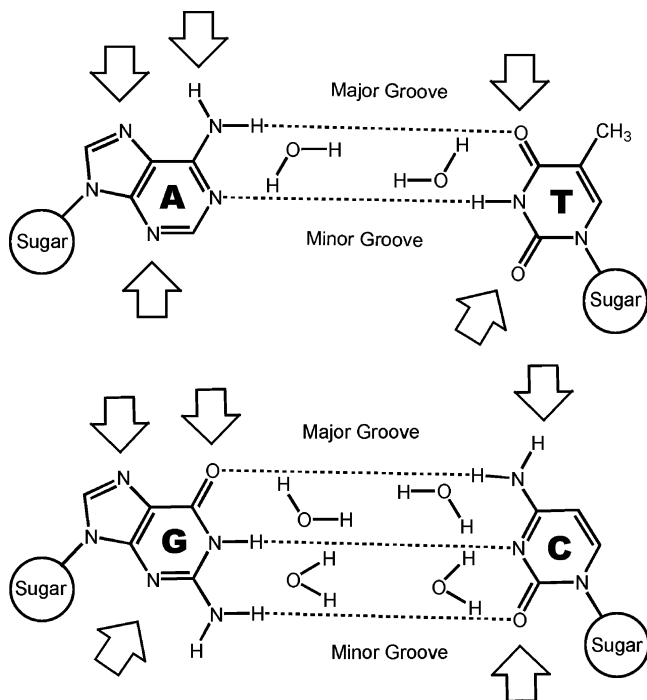
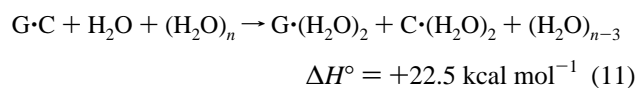
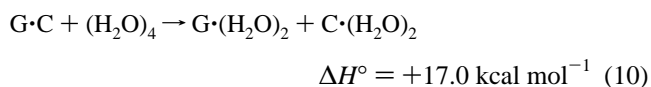
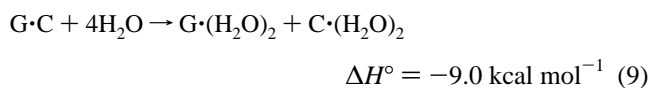
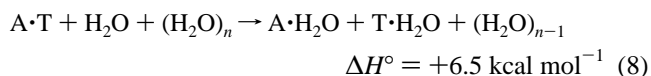
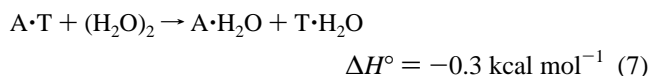
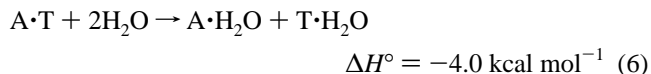


Figure 8. Schematic representation of possible nucleotide–nucleotide and nucleotide–water interactions. The dotted lines indicate Watson–Crick A–T and G–C base pairing interactions with the location of B-DNA minor and major grooves labeled correspondingly. Hydration sites set free upon breaking Watson–Crick hydrogen bonds are indicated by H–O–H symbols. Other hydration sites are pointed out by arrows.

base sequence to form a helical duplex. The two bases of the complementary Watson–Crick pairs A–T and G–C are held together by two and three hydrogen bonds, respectively, with calculated interaction enthalpies of 14.0 kcal mol⁻¹ for A–T and 27.0 kcal mol⁻¹ for G–C²⁸ or 7–9 kcal mol⁻¹ per hydrogen bond. The experimental base pair binding enthalpies of 13.0 (A–T) and 21.0 kcal mol⁻¹ (G–C)²⁹ cannot be considered a measure of the Watson–Crick interaction as population of the Watson–Crick structures is believed to be <30%³⁰ in these experiments. The hydration sites set free upon breaking the Watson–Crick hydrogen bonds are schematically indicated in Figure 8 using H–O–H symbols.⁶ Note, that all of the water molecules occupying these sites form two hydrogen bonds to the base. Water binding energies for the various sites are calculated⁶ to be 8–12 kcal mol⁻¹ in general agreement with our experimental values of ~9 kcal mol⁻¹ (see above). These values yield a base–water hydrogen bond strength of 4–6 kcal mol⁻¹, a value considerably smaller than the 7–9 kcal mol⁻¹ for a base–base hydrogen bond.

The process of breaking the A–T base pair with subsequent hydration of both A and T by one water molecule (eq 6) is exothermic by 4 kcal mol⁻¹.³¹ However, part of the exothermicity is due to a condensation process with three gas-phase particles (A·T + 2 H₂O) reacting to form two particles (A·H₂O + T·H₂O). This problem is eliminated when the reaction including a reactant water dimer (A·T + [H₂O]₂) is examined.³² The resulting process (eq 7) is thermoneutral indicating that base pairing is energetically a competitive

configuration. An alternative attempt to gauge the competition between hydration and base pairing is presented in reaction 8 with three gas-phase particles on both sides of the equation. Using an (H₂O)_n interaction energy of 10.5 kcal mol⁻¹ for large values of *n* (heat of evaporation²⁷) reaction 8 is endothermic with Watson–Crick A–T base pairing being clearly more stable than hydration of separated bases by 6.5 kcal mol⁻¹.



An analogous analysis for the G–C base pair (reactions 9–11) yields qualitatively the same result: base pairing is energetically a competitive process. In the G–C case, however, Watson–Crick base pairing is clearly more favorable than hydration by 20 kcal mol⁻¹ (reactions 10 and 11).³³

The discussion above is an attempt to understand how nucleobase molecules interact with each other and with individual water molecules and how strong the intrinsic interactions are. In the condensed phase all of the molecules considered here interact with additional molecules surrounding them. Hence, in aqueous solution or in the living organism a range of additional terms that depend on the nature of the surrounding material (aqueous, nonaqueous, hydrophilic, hydrophobic) determine the thermochemistry of breaking a base pair.

Water molecules bound to functional groups marked with arrows in Figure 8 do not directly compete with Watson–Crick base pairing. X-ray studies of B-form duplex model systems indicate that the functional groups marked by an arrow (Figure 8) point toward the minor and major grooves of the B-helix^{34,35} and are therefore available for hydration. In these studies several water oxygen atoms per nucleotide are explicitly observed as part of the crystal structure.³⁵ The most probable locations for the crystal water molecules coincide with the sites marked with arrows in Figure 8. Some crystal water molecules bridge the two strands of the double helix, a phenomena most prominent in the minor groove of A–T-rich parts of the B-DNA.^{34,36,37}

(28) Jurecka, P.; Hobza, P. *J. Am. Chem. Soc.* **2003**, *125*, 15608.

(29) Yanson, I. K.; Teplitsky, A. B.; Sukhodub, L. F. *Biopolymers* **1979**, *18*, 1149.

(30) Kabelac, M.; Hobza, P. *J. Phys. Chem. B* **2001**, *105*, 5804.

(31) 14 kcal mol⁻¹ (A–T) minus 2 × 9 kcal mol⁻¹ (base–water).

(32) (H₂O)₂ binding energy is 3.7 kcal mol⁻¹: Fellers R. S.; Leforestier, C.; Braly, L. B.; Brown, M. G.; Saykally, R. J. *Science* **1999**, *284*, 945.

(33) Water binding energy in (H₂O)₂ is 26.0 kcal mol⁻¹: Graf, S.; Leutwyler, S. *J. Chem. Phys.* **1998**, *109*, 5393.

(34) Jeffrey, G. A. *An introduction to hydrogen bonding*; Oxford University Press: New York, 1997.

(35) Schneider, B.; Cohen, D.; Berman, H. M. *Biopolymers* **1992**, *32*, 725.

NMR experiments indicate that the bridging water molecules forming a “spine of hydration” in the minor groove have residence times exceeding 1 ns.^{38,39} It is speculated³⁶ that those water molecules in bridging positions contribute to the stability of the B-helix relative to the A-helix, a less common form of double-stranded DNA, because low humidity promotes the A-form of DNA.² High G/C base content is also considered to be a factor contributing to the stability of A-DNA.⁴⁰

The negatively charged phosphate groups along the DNA double helix backbone are fully exposed to the solvent water. Hydrated counterions present in solution (e.g., Na^+_{aq}) move freely around the DNA molecule without being bound to specific sites on the backbone or elsewhere.⁴¹ Phosphate hydration is very dynamic and undetectable by NMR methods. However, a systematic analysis of water distributions around the phosphates found in DNA helical crystal structures indicates that the phosphate groups are more extensively hydrated than the bases but that the phosphate hydration shell is less organized than hydration of the bases.⁴² It is found that each of the nonbridging phosphate oxygen atoms O_{NBO} (see Scheme 1) is hydrated by three water molecules in the first solvation shell forming a “cone of hydration”.⁴² Our molecular mechanics studies on hydrated mononucleotides, $[\text{M}-\text{H}]^-(\text{H}_2\text{O})_4$, confirm extensive hydration of the phosphate group. Isomers with four water molecules bound to the phosphate group (see Figure 5b) are energetically competitive. The example displayed in Figure 5b shows an $(\text{H}_2\text{O})_3$ cone of hydration around one of the phosphate oxygen atoms.

Extensive phosphate hydration is also expected on the basis of the large phosphate–water interaction energy. Our experimental data indicate the first water molecule is bound by 11 and the following water molecules by 9 kcal mol⁻¹ (Table 1). Hence a cone of hydration of six water molecules amounts to 56 kcal mol⁻¹, comparable to the corresponding water–water interaction of 55 kcal mol⁻¹ in $(\text{H}_2\text{O})_7$.⁴³ Crystal structure X-ray studies indicate that the extensive hydration observed for the O_{NBO} oxygens does not extend to the phosphate ester oxygens. Very poor hydration is found for the $\text{O}3'$ and $\text{O}5'$ atoms of polynucleotides.^{37,42} Our molecular mechanics simulations on $[\text{M}-\text{H}]^-(\text{H}_2\text{O})_4$ mononucleotides indicate $\text{O}5'$ ester oxygen hydration is less favorable than hydration of the O_{NBO} oxygen atoms, but water coordination to $\text{O}5'$ is still observed in several low energy structures (see, e.g., Figure 5a, c, and d). However, in all cases the water molecule bound to $\text{O}5'$ is also bound to

one of the O_{NBO} oxygen atoms (see Figure 5a, c, and d). In a fully hydrated phosphate group $(-\text{PO}_4^-)\cdot(\text{H}_2\text{O})_n$, $n \gg 6$, the bridging position of water seen in Figure 5a might be less favorable than the cone of hydration configuration making the ester oxygen atoms less hydrophilic for large values of n .

Deoxyribose is generally not considered an independent unit of DNA hydration,^{37,42} because in B-DNA the only hydrophilic group on the sugar, the 4' oxygen, usually shares water with the minor-groove hydrophilic base atom from a previous residue. In our molecular mechanics studies on hydrated mononucleotides, $[\text{M}-\text{H}]^-(\text{H}_2\text{O})_4$, water never binds to $\text{O}4'$ in any of the low-energy isomers confirming that the close $\text{O}4'-\text{H}_2\text{O}$ contact in B-DNA is the result of a strong base– H_2O interaction, with the sugar $\text{O}4'$ atom being a close accidental bystander. In mononucleotides, however, the deoxyribose sugar molecule has an additional hydrophilic group, the 3' hydroxyl group, which competes effectively for a water molecule in our mononucleotide $[\text{M}-\text{H}]^-(\text{H}_2\text{O})_4$ simulations (see, e.g., Figures 5d, 6, and 7). In the polymerized form of nucleotides the 3' hydroxyl group is absent due to a phosphate ester linkage to the adjacent nucleotide.

Conclusions

1. The first water molecule binds more strongly to all of the protonated and deprotonated mononucleotide ions than the second through fourth water molecules. Modeling indicates that the first water molecule adds to the charged site in all cases except for $[\text{dAMP}+\text{H}]^+$ where the charged site is inaccessible to the water molecule.

2. The second through fourth water molecules all have about the same binding energy (~ 9 kcal mol⁻¹) regardless of the nucleotide and regardless of whether the nucleotide is protonated or deprotonated. This result sharply contrasts with results on peptides where a monotonic decrease in binding energy is observed as each water is added.

3. Theory predicts that the second through fourth water molecules bind equally well to a number of functional groups on the mononucleotides including charge-proximate and charge-remote sites or to already bound water molecules in a second solvation shell.

Acknowledgment. We acknowledge the helpful discussions with Dr. John E. Bushnell regarding DFT calculations. The support of the National Science Foundation under Grant CHE-0503728 is gratefully acknowledged.

Supporting Information Available: Full refs 11 (AMBER 7) and 14 (GAUSSIAN 03) and coordinates and energies of the geometry-optimized B3YLP/6-311++G** structures are given. This material is available free of charge via the Internet at <http://pubs.acs.org>.

JA062418O

(36) Drew, H. R.; Dickerson, R. E. *J. Mol. Biol.* **1981**, *151*, 535.

(37) Kopka, M. L.; Fratini, A. V.; Drew, H. R.; Dickerson, R. E. *J. Mol. Biol.* **1983**, *163*, 129.

(38) Liepinsh, E.; Otting, G.; Wuthrich, K. *Nucleic Acids Res.* **1992**, *20*, 6549.

(39) Kubinec, M. G.; Wemmer, D. E. *J. Am. Chem. Soc.* **1992**, *114*, 8739.

(40) Foloppe, N.; MacKerell, A. D., Jr. *Biophys. J.* **1999**, *76*, 3206.

(41) Bour, P.; Andrushchenko, V.; Kabelac, M.; Maharaj, V.; Wieser, H. J. *Phys. Chem. B* **2005**, *109*, 20579.

(42) Schneider, B.; Patel, K.; Berman, H. M. *Biophys. J.* **1998**, *75*, 2422.

(43) Su, J. T.; Xu, X.; Goddard, W. A., III. *J. Phys. Chem. A* **2004**, *108*, 10518.